

3. DATA REPORT: GEOCHEMICAL ANALYSES OF MASSIVE SULFIDE AND SEDIMENT SAMPLES FROM THE TAG HYDROTHERMAL MOUND¹

D. Jay Miller²

ABSTRACT

Bulk-rock geochemical analyses were performed on 29 samples of massive sulfide and sulfide-bearing sediment from the TAG hydrothermal mound. This pilot study was intended to determine whether or not enrichments of platinum group elements could be detected within the mound deposits. Although significant enrichments of Au were detected from near the surface of the mound and in at least one sample from within the mound, Pt concentrations were below the detection limit of the analytical method used. Pd concentrations in all samples were near or below detection limits as well. These data are included in this volume to complement other bulk-rock analyses and petrographic descriptions.

INTRODUCTION

Five different parts of the Trans-Atlantic Geotraverse (TAG) active hydrothermal mound were sampled during Leg 158 of the Ocean Drilling Program (ODP). The shorthand nomenclature for these locations adopted in Humphris, Herzig, Miller, et al. (1996) will be used in this report (see Fig. 1). This study was undertaken in order to assess the occurrence and distribution of platinum-group elements (PGE) within the TAG hydrothermal mound. Analysis of hydrothermal precipitates from the TAG mound has demonstrated a two to three orders of magnitude enrichment of Au relative to mid-ocean ridge basalt (Crocket, 1989, 1990; Hannington et al., 1991). Ravizza et al. (1996) report variable Os isotopic signatures for samples from the TAG mound, indicating that the Os in TAG sulfides could have been derived from either seawater or oceanic crust, or some combination of these two sources. Brüggemann et al. (Chap. 7, this volume) also recognize a range in Os isotope compositions, but with the additional sample depth control afforded by drilling they interpret a stratigraphic correlation. Samples with the highest Os isotope ratios (indicating Os derived from seawater) are those recovered from near the upper part of the mound; samples with lower Os isotope ratios were recovered from deeper in the mound (indicating a contribution of Os from the underlying basalt). These data suggest that the hydrothermal fluids present at TAG are capable of leaching chalcophile elements from basalt and transporting these elements to sulfide deposits at the seafloor. Concentrations of PGE have not, however, been reported for samples dredged or collected by submersible from the TAG mound. The sampling strategy for this pilot study was to collect samples of Cu-rich sulfides from various horizons within the mound to determine if there were subsurface concentrations of PGE.

SAMPLE DESCRIPTIONS

Because Pt and Pd are chalcophile elements commonly associated with sulfide minerals, samples were selected for analysis that were representative of the main sulfide-bearing mineralogies sampled. The terminology used to describe the major lithologic units is the same as used during Leg 158 (Humphris, Herzig, Miller, et al., 1996). Particular care was taken to sample where concentrations of chalcopyrite

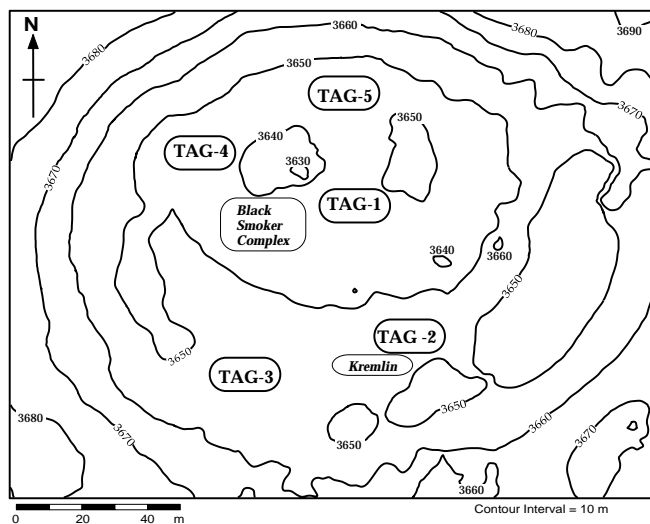


Figure 1. Sketch bathymetry map of the active TAG hydrothermal mound derived from 120 kHz, side-scan sonar data (Kleinrock et al., 1996). This map shows the general position of the five locations sampled during Leg 158.

were high (relative to the ubiquitous pyrite) and gangue minerals (anhydrite and silica) were low. Therefore, even samples named pyrite-silica-anhydrite breccia were taken from the most sulfide-rich, but silica- and anhydrite-poor, parts of the core. In the pilot study, 20 samples of porous to massive sulfide and sulfide-bearing breccias and sands were analyzed. Table 1 summarizes petrographic observations from these samples. After determining that these samples were barren (or nearly so) of platinum-group elements at the analytical threshold, but recognizing that samples from the shallowest cores had elevated Au contents, another nine samples taken from within ~30 cm of the tops of cores were analyzed for Au, Pt, and Pd. Two of these samples were of sufficient volume to analyze for major element oxides and trace elements as well.

ANALYTICAL METHODS

For bulk-rock analysis of major element oxides and some trace elements, an aliquot of the powdered sample was prepared using LiBO₂ fusion (at 1025°C for 25 min), followed by acid digestion (HNO₃) and analysis by an inductively coupled plasma emission spectrograph (ICP-ES). Two duplicate analyses were run to monitor analytical pre-

¹Herzig, P.M., Humphris, S.E., Miller, D.J., and Zierenberg, R.A. (Eds.), 1998. *Proc. ODP, Sci. Results, 158*: College Station, TX (Ocean Drilling Program).

²Ocean Drilling Program, Texas A&M University Research Park, 1000 Discovery Drive, College Station, TX 77845, U.S.A. Jay_Miller@odp.tamu.edu

Table 1. Petrographic summaries of massive sulfide and sulfide breccias.

Core, section, interval top (cm)	Petrographic summary
957B-1R-2, 16	Massive granular pyrite. 97% pyrite, 3% silica. Aggregates of medium to coarse euhedral grains.
957C-7N-2, 68	Pyrite-silica-anhydrite breccia. 55% pyrite, 35% anhydrite, 15% silica, 5% chalcopyrite. Fine-grained, clast-supported breccia with nodular pyrite embedded in an anhydrite matrix with subordinate gray chert.
957C-11N-1, 32	Pyrite-anhydrite breccia. 75% pyrite, 15% anhydrite, 10% chalcopyrite. Chalcopyrite is concentrated near anhydrite veins. Pyrite is fine grained, with some rounded grains and aggregates.
957C-11N-3, 116	Pyrite-silica-anhydrite breccia. 40% pyrite, 25% silica, 25% anhydrite, 10% chalcopyrite. Pyrite has seriate grain-size distribution, fine to medium coarse grained. Chalcopyrite is concentrated along vein selvage. Small altered basalt clasts are present.
957C-12N-2, 91	Pyrite-anhydrite breccia. 50% pyrite, 30% anhydrite, 20% chalcopyrite. Nodular fine-grained clasts of pyrite. Chalcopyrite is concentrated along anhydrite veins.
957C-13N-1, 134	Pyrite-silica-anhydrite breccia. 70% pyrite, 15% anhydrite, 5% silica, 10% chalcopyrite. Fine-grained pyrite in matrix of anhydrite and silica. Chalcopyrite is most abundant along anhydrite veins.
957C-14N-1, 43	Massive pyrite-chalcopyrite. 55% pyrite, 30% chalcopyrite, 15% anhydrite. Fine-grained pyrite and chalcopyrite with thin anhydrite veins.
957C-16N-2, 91	Silicified wallrock breccia. 55% pyrite, 35% silica, 5% anhydrite, 5 chalcopyrite. Silicified basalt fragments with abundant fine-grained euhedral pyrite. Porous clast-supported breccia.
957E-4R-1, 5	Silicified wallrock breccia. 45% pyrite, 20% silica, 15% anhydrite, 20% chalcopyrite. Anhydrite and chalcopyrite along vein selvage. Pyritized and silicified basalt fragments are common.
957F-1N-1, 59	Pyrite-anhydrite breccia. 70% pyrite, 15% anhydrite, 10% chalcopyrite, 5% silica. Angular, medium-sized grains of chalcopyrite with variably sized pyrite (fine to coarse) grains in a clast-supported breccia with anhydrite matrix.
957G-1N-1, 23	Massive pyrite. 85% pyrite, 5% chalcopyrite, 5% anhydrite, 5% silica. Medium-grained, euhedral to colloform habit, a few percent of pore space is present. Silica and anhydrite appear to be filling pore spaces, may be very late filling.
957G-3N-1, 25	Pyrite breccia. 85% pyrite, 5% chalcopyrite, 5% anhydrite, 5% silica. Medium-grained, granular pyrite with relatively abundant chalcopyrite grains. Clast-supported breccia with silica matrix. Anhydrite is in thin veins.
957H-5N-1, 40	Pyrite-silica breccia. 75% pyrite, 15% silica, 5% anhydrite, 5% chalcopyrite. Rounded nodules of altered basalt that are now a mixture of gray silica and pyrite. Pyrite also occurs as rounded nodules. Chalcopyrite is embedded in pyrite nodules. Anhydrite is in veins and vugs.
957H-8N-1, 1	Pyrite-silica breccia. 80% pyrite, 20% silica. Rounded to angular pyrite and pyritized basalt fragments in a silica matrix. Clast-supported breccia.
957K-2N-1, 28	Pyrite-silica-anhydrite breccia. 70% pyrite, 20% anhydrite, 5% chalcopyrite, 5% silica. Rounded to subangular pyrite-chalcopyrite clasts in clast-supported breccia. Voids filled with anhydrite and amorphous silica.
957M-1R-2, 30	Pyrite-silica breccia. 60% pyrite, 35% silica, 5% chalcopyrite. Medium- to coarse-grained aggregates of pyrite occurring in altered basalt clasts and in matrix. Chalcopyrite is fine grained and disseminated with some accumulation along margins of altered basalt clasts.
957M-5R-1, 81	Silicified wallrock breccia. 73% pyrite, 25% silica, 2% chalcopyrite. Most pyrite-chalcopyrite-rich fragment of this piece. Fine-grained, disseminated pyrite in altered basalt clasts.
957P-1R-1, 1	Pyrite-anhydrite breccia. 50% pyrite, 40% anhydrite, 10% chalcopyrite. Fine, euhedral pyrite grains and rounded aggregates. Anhydrite in veins and in matrix of clast-supported breccia. Chalcopyrite abundant on vein selvages.
957P-4R-1, 5	Massive pyrite. 85% pyrite, 5% anhydrite, 5% silica, 5% chalcopyrite. Anhydrite and silica in vugs and fractures. Pyrite is euhedral and fine grained, with disseminated chalcopyrite.
957P-11R-1, 42	Pyrite-silica breccia. 80% pyrite, 10% silica, 5% anhydrite, 5% chalcopyrite. Pyrite is fine grained, disseminated in altered basalt clasts and in aggregates in silica matrix of clast-supported breccia. Anhydrite is in voids and vugs. Chalcopyrite is disseminated.

cision, one selected by the laboratory, and a second included as an additional unknown (see Tables 2, 3, and 4). A well-characterized laboratory standard material was also analyzed to evaluate analytical accuracy. These data are in Table 2. For trace-element analysis, a four-acid (HNO₃, HClO₄, HF, HCl) digestion was used, followed by ICP-ES analysis (Table 3). Ba and Sr were analyzed after both digestion methods, and values are included in Tables 2 and 3 for comparison. Loss on ignition (LOI) was determined by igniting a 1-g sample split at 950°C for 90 minutes and measuring weight loss. PGE analyses generally require processing large quantities of sample (±1 kg) in order to avoid unrepresentative analyses wherein the inclusion of a single PGE-bearing mineral grain in a small sample can bias the result. ODP sampling limitations precluded processing samples of this size, therefore the quantities homogenized for this study were on the order of 30 to 50 g. Au, Pt, and Pd concentrations were determined by fusion digestion of 30 g of sample, lead-collection fire assay, and analysis by ICP-ES (Table 4). This data set is provided to complement other bulk rock analytical data elsewhere in this volume. Analyses were performed by Acme Analytical Laboratories, Vancouver, B.C.

RESULTS

Samples analyzed in this study had Pt and Pd contents at or below detection limits. Significant Au concentrations were analyzed in several samples. Most of the Au-bearing samples were from the uppermost cores taken from the mound, the significant exception was ~700 ppb taken from a depth of 21 meters below seafloor (mbsf; Sample 158-957G-3N-1, 25 cm). A second series of analyses was performed on sulfide-bearing sands from uppermost parts of the core from the TAG-2, TAG-3, and TAG-4 locations. TAG-2 and TAG-3 samples all show elevated Au contents, but are still at or below detection limits for Pt and Pd. TAG-4 samples have only background levels of Au.

ACKNOWLEDGMENTS

The author thanks Editorial Review Board member Rob Zierenberg and an anonymous reviewer for their helpful comments. This work was supported by USSSP grant #158-20911B.

REFERENCES

- Crocket, J.H., 1989. PGE/Au fractionation in mid-ocean ridge volcanism. *Progr. with Abstr., Geol. Assoc. Can.*, 14:70.
- , 1990. Noble metals in seafloor hydrothermal mineralization from the Juan de Fuca and Mid-Atlantic ridges: a fractionation of gold from platinum metals in hydrothermal fluids. *Can. Mineral.*, 28:639–648.
- Hannington, M.D., Herzig, P.M., Scott, S.D., Thompson, G., and Rona, P.A., 1991. Comparative mineralogy and geochemistry of gold-bearing sulfide deposits on the mid-ocean ridges. *Mar. Geol.*, 101:217–248.
- Humphris, S.E., Herzig, P.M., Miller, D.J., et al., 1996. *Proc. ODP, Init. Repts.*, 158: College Station, TX (Ocean Drilling Program).
- Kleinrock, M.C., Humphris, S.E., and the Deep-TAG Team, 1996. Detailed structure and morphology of the TAG active hydrothermal mound and its geotectonic environment. In Humphris, S.E., Herzig, P.M., Miller, D.J., et al., *Proc. ODP, Init. Repts.*, 158: College Station, TX (Ocean Drilling Program), 15–21.
- Ravizza, G., Martin, C.E., German, C.R., and Thompson, G., 1996. Os isotopes as tracers in seafloor hydrothermal systems: metalliferous deposits from the TAG-hydrothermal area, 26°N Mid-Atlantic Ridge. *Earth. Planet. Sci. Lett.*, 138:105–119.

Date of initial receipt: 3 June 1996

Date of acceptance: 21 February 1997

Ms 158SR-204

Table 2. Geochemical analyses of samples from the TAG hydrothermal mound.

Core, section, interval (cm)	Component:	SiO ₂	TiO ₂	Al ₂ O ₃	Fe ₂ O ₃ ^T	MnO	MgO	CaO	Na ₂ O	K ₂ O	P ₂ O ₅	S ^T	LOI	Ba	Sr	Zr	
	Detection limit*:	0.01%	0.01%	0.01%	0.01%	0.01%	0.01%	0.01%	0.01%	0.04%	0.01%	0.1%	0.1%	5 ppm	10 ppm	10 ppm	
	Rock type	Location															
957B-1R-2, 16	Massive pyrite	TAG-2	2.84	0.03	0.85	63.27	bdl	0.01	0.13	0.16	0.04	0.14	53.4	33.1	9	bdl	60
957C-7N-2, 68	Pyrite-silica-anhydrite breccia	TAG-1	7.36	0.04	0.28	43.23	bdl	0.01	14.27	0.20	bdl	0.22	44.0	31.0	17	542	47
957C-11N-1, 32	Pyrite-anhydrite breccia	TAG-1	1.08	bdl	0.29	55.19	bdl	bdl	6.46	0.04	0.05	0.12	45.3	28.5	6	258	bdl
957C-11N-3, 116	Pyrite-silica-anhydrite breccia	TAG-1	24.64	0.15	0.88	36.64	bdl	0.18	9.09	0.09	0.04	0.20	33.2	24.1	16	397	bdl
	Split included as additional unknown		24.35	0.13	0.80	36.75	bdl	0.16	8.85	0.09	0.04	0.19	33.1	24.2	18	405	bdl
957C-12N-2, 91	Pyrite-anhydrite breccia	TAG-1	1.06	bdl	0.41	40.37	bdl	0.23	11.39	bdl	bdl	0.21	44.5	29.4	bdl	443	bdl
957C-13N-1, 134	Pyrite-silica-anhydrite breccia	TAG-1	3.11	0.01	0.24	50.10	bdl	0.08	6.46	bdl	0.04	0.14	51.6	29.2	25	275	17
957C-14N-1, 43	Massive pyrite-chalcopyrite	TAG-1	1.30	0.02	0.36	41.41	bdl	0.20	5.87	bdl	bdl	0.37	41.1	23.5	19	214	bdl
957C-16N-2, 91	Silicified wallrock breccia	TAG-1	32.90	0.17	1.66	39.84	bdl	0.25	2.15	0.09	0.05	0.19	35.8	21.8	18	99	32
957E-4R-1, 5	Silicified wallrock breccia	TAG-1	19.31	0.04	0.31	41.92	bdl	0.09	5.93	bdl	0.04	0.32	37.0	22.7	17	252	34
957F-1N-1, 59	Pyrite-anhydrite breccia	TAG-1	6.05	0.04	0.48	50.07	bdl	0.15	5.73	0.01	0.04	0.24	48.3	31.2	8	282	29
957G-1N-1, 23	Massive pyrite	TAG-1	6.01	bdl	0.25	57.92	bdl	0.02	1.36	bdl	bdl	0.11	52.6	31.1	12	61	41
957G-3N-1, 25	Pyrite breccia	TAG-1	1.61	0.04	0.20	61.23	bdl	0.03	1.08	bdl	bdl	0.08	55.9	32.2	bdl	58	13
957H-5N-1, 40	Pyrite-silica breccia	TAG-2	16.68	0.12	1.01	48.09	bdl	0.36	3.41	0.19	0.16	0.49	46.0	27.0	57	69	42
957H-8N-1, 1	Pyrite-silica breccia	TAG-2	18.03	0.07	0.55	52.21	bdl	0.05	0.43	bdl	0.04	0.13	45.7	28.2	6	25	215
957K-2N-1, 28	Pyrite-silica-anhydrite breccia	TAG-4	6.79	0.04	0.32	48.81	0.01	0.03	8.90	bdl	0.04	0.28	49.7	30.9	bdl	496	76
957M-1R-2, 30	Pyrite-silica breccia	TAG-4	30.72	0.18	0.82	42.74	bdl	0.06	2.60	0.05	0.04	0.09	39.2	21.0	44	149	68
957M-5R-1, 81	Silicified wallrock breccia	TAG-4	25.17	0.19	1.68	46.55	bdl	0.07	0.31	0.17	0.06	0.08	41.7	24.6	47	27	61
	Laboratory-selected repeat analysis		24.81	0.16	1.64	46.47	bdl	0.05	0.29	0.18	0.06	0.05	40.8	24.5	32	26	59
957P-1R-1, 1	Pyrite-anhydrite breccia	TAG-5	2.47	0.04	0.42	35.53	bdl	0.04	15.30	0.04	0.04	0.25	39.4	20.5	25	836	163
957P-4R-1, 5	Massive pyrite	TAG-5	7.50	bdl	0.44	58.04	bdl	0.02	1.80	bdl	0.04	0.20	53.2	29.4	20	93	30
957P-11R-1, 42	Pyrite-silica breccia	TAG-5	11.59	0.01	0.25	55.65	bdl	0.03	1.33	bdl	bdl	0.05	51.2	28.0	bdl	80	29
957Q-1R-1, 20	Sulfide-bearing sand	TAG-3	47.89	0.01	0.06	26.51	0.01	0.10	0.12	0.35	0.04	bdl	22.9	13.8	5	12	bdl
957Q-1R-1, 30	Sulfide-bearing sand	TAG-3	23.99	bdl	0.04	36.93	0.01	0.07	0.07	0.29	bdl	bdl	36.0	20.9	3	7	bdl
957Q-1R-3, 48	Sulfide-bearing sand	TAG-3	17.37	0.04	0.25	49.35	bdl	0.06	0.55	0.16	0.04	0.27	42.2	24.3	17	33	10
Standard SO-15	As analyzed with this sample set		50.92	2.81	12.69	7.47	1.38	7.14	5.84	2.31	1.78	2.81			2176	380	760
	Average composition of this standard		49.24	1.64	12.73	7.23	1.36	7.19	5.83	2.41	1.97	2.79			2189	385	733

Notes: * = provided by Acme Analytical Laboratories, using 95% confidence limits; bdl = below detection limit. Single acid digestion used in sample preparation.

Table 3. Trace element analyses of samples from the TAG hydrothermal mound.

Core, section, interval (cm)	Component:	Cu	Zn	Pb	Cd	Ag	Ni	Mo	Co	Mn	Fe	As	U	Th	
	Detection limit*:	2 ppm	2 ppm	5 ppm	0.4 ppm	0.5 ppm	2 ppm	2 ppm	2 ppm	5 ppm	0.01%	5 ppm	10 ppm	2 ppm	
	Rock type	Location													
957B-1R-2, 16	Massive pyrite	TAG-2	592	36	29	bdl	1.0	7	60	216	63	42.68	bdl	18	3
957C-7N-2, 68	Pyrite-silica-anhydrite breccia	TAG-1	20,037	235	27	0.9	1.3	12	48	139	bdl	26.17	bdl	bdl	3
957C-11N-1, 32	Pyrite-anhydrite breccia	TAG-1	34,395	905	26	2.5	1.4	3	88	109	26	34.60	bdl	11	bdl
957C-11N-3, 116	Pyrite-silica-anhydrite breccia	TAG-1	26,876	162	13	1.7	0.8	10	35	206	5	22.33	bdl	bdl	bdl
	Split included as additional unknown		26,768	150	15	2.1	0.8	12	36	201	9	22.55	bdl	bdl	bdl
957C-12N-2, 91	Pyrite-anhydrite breccia	TAG-1	73,683	312	8	5.0	1.7	bdl	58	155	47	27.68	bdl	bdl	2
957C-13N-1, 134	Pyrite-silica-anhydrite breccia	TAG-1	38,223	289	24	1.8	1.2	4	76	167	bdl	33.64	bdl	bdl	2
957C-14N-1, 43	Massive pyrite-chalcopyrite	TAG-1	>100,000	254	bdl	9.3	1.6	bdl	66	114	10	30.38	bdl	bdl	3
957C-16N-2, 91	Silicified wallrock breccia	TAG-1	10,873	67	8	bdl	bdl	16	30	459	19	26.31	bdl	bdl	bdl
957E-4R-1, 5	Silicified wallrock breccia	TAG-1	66,752	134	bdl	4.8	1.7	bdl	73	168	29	26.66	bdl	12	5
957F-1N-1, 59	Pyrite-anhydrite breccia	TAG-1	38,481	434	18	0.9	2.9	5	68	290	11	31.73	bdl	13	2
957G-1N-1, 23	Massive pyrite	TAG-1	20,708	853	28	1.4	1.2	2	66	97	22	38.19	bdl	10	bdl
957G-3N-1, 25	Pyrite breccia	TAG-1	20,037	3,309	73	6.9	11.4	10	66	169	16	40.47	13	25	bdl
957H-5N-1, 40	Pyrite-silica breccia	TAG-2	11,968	254	17	1.1	0.7	12	43	364	28	33.79	bdl	bdl	bdl
957H-8N-1, 1	Pyrite-silica breccia	TAG-2	5,462	1,025	55	1.2	2.9	8	67	315	16	35.63	5	bdl	3
957K-2N-1, 28	Pyrite-silica-anhydrite breccia	TAG-4	24,434	308	26	1.8	2.1	7	52	134	19	30.07	bdl	15	bdl
957M-1R-2, 30	Pyrite-silica breccia	TAG-4	9,897	289	22	bdl	1.5	12	32	227	26	27.45	bdl	bdl	2
957M-5R-1, 81	Silicified wallrock breccia	TAG-4	7,646	4,262	42	8.0	3.1	12	60	253	9	31.37	bdl	18	3
	Laboratory-selected repeat analysis		7,687	4,242	51	9.7	3.2	17	60	257	16	31.62	bdl	21	bdl
957P-1R-1, 1	Pyrite-anhydrite breccia	TAG-5	37,760	432	bdl	3.8	0.6	8	61	129	bdl	23.35	bdl	bdl	4
957P-4R-1, 5	Massive pyrite	TAG-5	15,296	610	50	3.6	2.2	7	70	207	34	36.91	bdl	40	4
957P-11R-1, 42	Pyrite-silica breccia	TAG-5	22,023	734	62	1.6	2.1	6	104	316	14	35.92	bdl	33	bdl
957Q-1R-1, 20	Sulfide-bearing sand	TAG-3	59,386	7,598	138	26.1	6.0	10	34	41	130	18.23	5	bdl	bdl
957Q-1R-1, 30	Sulfide-bearing sand	TAG-3	87,376	6,599	118	30.4	5.0	8	49	78	67	26.33	bdl	bdl	bdl
957Q-1R-3, 48	Sulfide-bearing sand	TAG-3	51,078	2,851	40	11.3	2.3	8	44	118	33	33.02	13	17	bdl
Standard CT/FA-100S	As analyzed with this sample set		59	128	36	16.2	6.4	68	18	29	1170	4.10	28	22	43
	Average composition of this standard		59	148	40	18.5	6.0	76	20	33	1176	4.37	35	20	41

Notes: * = provided by Acme Analytical Laboratories, using 95% confidence limits. bdl = below detection limit. Four-acid digestion used in sample preparation.

Table 3 (continued).

Core, section, interval (cm)	Component:	Sr	Sb	Bi	V	Ca	La	Ba	Ti	Al	Na	Sn	Nb	Be	Sc	
	Detection limit*:	2 ppm	5 ppm	5 ppm	2 ppm	0.01%	2 ppm	1 ppm	0.01%	0.01%	0.01%	2 ppm	2 ppm	1 ppm	1 ppm	
	Rock type	Location														
957B-1R-2, 16	Massive pyrite	TAG-2	3	5	8	11	0.08	bdl	10	bdl	0.39	0.12	4	3	2	bdl
957C-7N-2, 68	Pyrite-silica-anhydrite breccia	TAG-1	480	bdl	16	2	8.19	bdl	3	bdl	0.07	0.10	3	bdl	bdl	bdl
957C-11N-1, 32	Pyrite-anhydrite breccia	TAG-1	237	9	27	3	3.88	bdl	4	bdl	0.11	0.04	3	bdl	bdl	bdl
957C-11N-3, 116	Pyrite-silica-anhydrite breccia	TAG-1	386	8	11	11	5.72	bdl	6	0.01	0.35	0.07	3	bdl	1	1
	Split included as additional unknown		393	7	14	15	5.65	bdl	3	bdl	0.35	0.06	3	bdl	bdl	bdl
957C-12N-2, 91	Pyrite-anhydrite breccia	TAG-1	426	14	47	7	7.00	bdl	4	bdl	0.16	0.03	11	bdl	bdl	bdl
957C-13N-1, 134	Pyrite-silica-anhydrite breccia	TAG-1	255	bdl	17	2	3.93	bdl	2	bdl	0.08	0.03	2	bdl	bdl	bdl
957C-14N-1, 43	Massive pyrite-chalcopyrite	TAG-1	213	16	95	9	3.81	bdl	2	bdl	0.13	0.02	14	bdl	bdl	bdl
957C-16N-2, 91	Silicified wallrock breccia	TAG-1	97	bdl	7	23	1.42	bdl	2	0.05	0.76	0.15	bdl	3	2	2
957E-4R-1, 5	Silicified wallrock breccia	TAG-1	243	bdl	34	2	3.73	bdl	2	bdl	0.09	0.02	6	bdl	bdl	bdl
957F-1N-1, 59	Pyrite-anhydrite breccia	TAG-1	248	bdl	17	10	3.26	bdl	2	bdl	0.19	0.03	bdl	bdl	bdl	bdl
957G-1N-1, 23	Massive pyrite	TAG-1	56	bdl	10	16	0.85	bdl	1	bdl	0.09	0.02	2	2	bdl	bdl
957G-3N-1, 25	Pyrite breccia	TAG-1	51	19	18	9	0.68	bdl	1	bdl	0.08	0.02	3	bdl	bdl	bdl
957H-5N-1, 40	Pyrite-silica breccia	TAG-2	48	bdl	12	19	0.66	bdl	1	0.01	0.38	0.08	3	2	1	1
957H-8N-1, 1	Pyrite-silica breccia	TAG-2	23	bdl	18	9	0.27	bdl	bdl	bdl	0.23	0.04	3	bdl	bdl	bdl
957K-2N-1, 28	Pyrite-silica-anhydrite breccia	TAG-4	439	bdl	11	8	5.09	bdl	5	0.01	0.11	0.04	bdl	bdl	bdl	bdl
957M-1R-2, 30	Pyrite-silica breccia	TAG-4	142	5	bdl	19	1.65	bdl	4	0.01	0.31	0.05	bdl	3	bdl	bdl
957M-5R-1, 81	Silicified wallrock breccia	TAG-4	19	bdl	5	28	0.14	bdl	36	0.06	0.74	0.14	3	4	3	3
	Laboratory-selected repeat analysis		18	14	9	29	0.13	bdl	32	0.07	0.76	0.15	bdl	bdl	8	3
957P-1R-1, 1	Pyrite-anhydrite breccia	TAG-5	763	bdl	20	8	9.13	bdl	6	bdl	0.14	0.06	bdl	bdl	bdl	bdl
957P-4R-1, 5	Massive pyrite	TAG-5	82	bdl	18	10	1.08	bdl	bdl	bdl	0.15	0.03	bdl	bdl	bdl	bdl
957P-11R-1, 42	Pyrite-silica breccia	TAG-5	73	5	17	2	0.80	bdl	bdl	bdl	0.06	0.02	bdl	bdl	bdl	bdl
957Q-1R-1, 20	Sulfide-bearing sand	TAG-3	12	23	18	33	0.09	bdl	5	bdl	0.04	0.25	4	bdl	3	bdl
957Q-1R-1, 30	Sulfide-bearing sand	TAG-3	7	29	41	19	0.06	bdl	3	bdl	0.03	0.21	7	bdl	bdl	bdl
957Q-1R-3, 48	Sulfide-bearing sand	TAG-3	27	18	49	10	0.32	bdl	bdl	bdl	0.05	0.13	5	bdl	bdl	bdl
Standard CT/FA-100S	As analyzed with this sample set		235	27	18	100	1.08	43	917	0.34	6.23	1.44	17	7	bdl	13
	Average composition of this standard		239	22	17	135	1.16	45	832	0.33	7.27	1.66	19	8	2	15

Table 4. Precious metal concentrations in samples from the TAG hydrothermal mound.

Hole, core, section, interval (cm)	Component:		Au	Pt	Pd
	Detection limit*:		2 ppb	3 ppb	3 ppb
	Rock type	Location			
957B-1R-1, 11	Sulfide-bearing sand	TAG-2	2797	bdl	bdl
957B-1R-1, 21	Sulfide-bearing sand	TAG-2	1823	bdl	bdl
957B-1R-1, 30	Sulfide-bearing sand	TAG-2	1909	bdl	bdl
957B-1R-2, 16	Massive pyrite	TAG-2	71	bdl	5
957C-7N-2, 68	Pyrite-silica-anhydrite breccia	TAG-1	103	bdl	3
957C-11N-1, 32	Pyrite-anhydrite breccia	TAG-1	72	bdl	4
957C-11N-3, 116	Pyrite-silica-anhydrite breccia	TAG-1	48	bdl	3
	Split included as additional unknown		46	bdl	3
957C-12N-2, 91	Pyrite-anhydrite breccia	TAG-1	83	bdl	4
957C-13N-1, 134	Pyrite-silica-anhydrite breccia	TAG-1	46	bdl	3
957C-14N-1, 43	Massive pyrite-chalcopyrite	TAG-1	43	bdl	5
957C-16N-2, 91	Silicified wallrock breccia	TAG-1	14	bdl	4
957E-4R-1, 5	Silicified wallrock breccia	TAG-1	39	bdl	4
957F-1N-1, 59	Pyrite-anhydrite breccia	TAG-1	222	bdl	4
957G-1N-1, 23	Massive pyrite	TAG-1	309	bdl	3
957G-3N-1, 25	Pyrite breccia	TAG-1	699	bdl	4
957H-5N-1, 40	Pyrite-silica breccia	TAG-2	128	bdl	5
957H-8N-1, 1	Pyrite-silica breccia	TAG-2	193	bdl	3
957K-2N-1, 28	Pyrite-silica-anhydrite breccia	TAG-4	227	bdl	5
957M-1R-1, 9	Sulfide-bearing sand	TAG-4	93	bdl	bdl
957M-1R-1, 21	Sulfide-bearing sand	TAG-4	65	bdl	bdl
957M-1R-1, 33	Sulfide-bearing sand	TAG-4	24	bdl	bdl
957M-1R-2, 30	Pyrite-silica breccia	TAG-4	154	bdl	5
957M-5R-1, 81	Silicified wallrock breccia	TAG-4	223	bdl	3
	Laboratory-selected repeat analysis		223	bdl	4
957P-1R-1, 1	Pyrite-anhydrite breccia	TAG-5	103	bdl	bdl
957P-4R-1, 5	Massive pyrite	TAG-5	189	bdl	bdl
957P-11R-1, 42	Pyrite-silica breccia	TAG-5	268	bdl	4
957Q-1R-1, 20	Sulfide-bearing sand	TAG-3	1171	bdl	bdl
957Q-1R-1, 30	Sulfide-bearing sand	TAG-3	1217	bdl	bdl
957Q-1R-3, 48	Sulfide-bearing sand	TAG-3	737	bdl	3
Standard CT/FA-100S	As analyzed with this sample set		44	46	45
	Average composition of this standard		49	46	46

Note: * = provided by Acme Analytical Laboratories, using 95% confidence limits; bdl = below detection limit.